



Published in final edited form as:

*J Thorac Oncol.* 2015 June ; 10(6): 951–959. doi:10.1097/JTO.0000000000000545.

## Primary Pulmonary NUT-Midline Carcinoma: Clinical, Radiographic, and Pathologic Characterization

Lynette M. Sholl, M.D.<sup>1</sup>, Mizuki Nishino, M.D.<sup>2</sup>, Saraswati Pokharel, M.D., Ph.D.<sup>3</sup>, Mari Mino-Kenudson, M.D.<sup>4</sup>, Christopher A. French, M.D.<sup>1</sup>, Pasi A. Janne, M.D., Ph.D.<sup>5</sup>, and Christopher Lathan, M.D., M.P.H.<sup>5</sup>

<sup>1</sup> Brigham and Women's Hospital, Department of Pathology, Boston, MA

<sup>2</sup> Dana Farber Cancer Institute, Department of Imaging, Boston, MA

<sup>3</sup> Roswell Park Cancer Institute, Department of Pathology and Laboratory Medicine, Buffalo, NY

<sup>4</sup> Massachusetts General Hospital, Department of Pathology, Boston, MA

<sup>5</sup> Dana Farber Cancer Institute, Thoracic Oncology Program, Boston, MA

### Abstract

NUT midline carcinoma (NMC) is a poorly differentiated tumor typically driven by a t(15;19) rearrangement leading to a *NUT* fusion event. This rare and uniformly fatal tumor arises in multiple organ sites, however the clinical, radiographic, and pathologic characteristics of primary pulmonary NMC are poorly defined. We identified eight cases of primary pulmonary NMC in our consult practice over four years and, using a NUT immunohistochemistry screen, retrospectively identified one additional case from 166 (0.6%) consecutive in-house biopsies of lung carcinomas lacking glandular differentiation. Eight cases had available clinical and radiographic data and shared a remarkable degree of similarity. The median age at presentation was 30 (range 21-68). Six patients had little or no smoking history. All complained of one to three months of cough at presentation. Computed tomography scans showed a large, centrally-located primary mass with confluent involvement of mediastinal lymph nodes, pleural disease, and sparing of the contralateral lung. Lytic bone metastases were common but brain metastases were absent in all cases. Pathologically, all cases showed primitive-appearing round to epithelioid cells growing in nests and sheets. All tumors expressed keratin, p63 or p40, and NUT protein. Eight cases had a FISH-proven *BRD4-NUT* or *BRD3-NUT* rearrangement; one case was presumed to have a NUT-variant fusion event. Median overall survival was 2.2 months. Despite the rarity of primary pulmonary NMC, it is important to recognize this entity in order to counsel patients regarding outcome and to identify candidates for targeted BRD inhibitors currently in clinical trials.

### Keywords

NUT-midline carcinoma; pulmonary; squamous cell carcinoma

## Introduction

NUT-midline carcinoma (NMC) is a highly aggressive tumor defined by a rearrangement involving the *NUTM1* (*Nut midline carcinoma, family member 1, NUT*) gene on chromosome 15 and sharing some histopathologic features with squamous cell carcinomas. This rearrangement leads to the fusion of *NUT* to one of a number of possible partners including the bromodomain family members BRD3 or BRD4 or the methyltransferase, NSD3, leading to global epigenetic reprogramming and loss of cell differentiation.<sup>1-5</sup> The tumor has been reported to arise in many sites, although the largest series suggest a predilection for the head and neck and mediastinum.<sup>6,7</sup> NMC is extremely aggressive, with most cases presenting at an advanced stage and progressing rapidly to death. The estimated 2 year progression free survival is 9%, based on studies incorporating all sites of disease.<sup>8</sup>

Large series describing NMC in the lung are lacking, but existing literature suggests that primary pulmonary NMC is exceptionally rare. Tanaka et al. described only two cases of probable lung origin in a survey of 41 years of cases gathered from their institution, both in pediatric patients.<sup>9</sup> Haruki et al. derived the cell line HCC2429 from a metastatic lung carcinoma proven to contain the t(15;19) translocation, but were unable to identify any additional cases of NMC from a series of 128 lung carcinomas screened by fluorescence in situ hybridization for this translocation.<sup>10</sup>

Pathologically, NMC is characterized by often monomorphic, primitive-appearing tumor cells frequently lacking the protein expression profiles characteristic of common carcinomas, however cases can show squamous differentiation in the form of focal, abrupt keratinization and/or expression of high molecular weight cytokeratins and lineage-specific transcription factors such as p63 and p40 (Np63).<sup>7,11</sup> The undifferentiated nature of NMC leads to difficulty in morphologic recognition, and thus the differential diagnosis is broad, including poorly differentiated non small cell carcinoma, small cell lung carcinoma, round cell sarcomas, and high grade lymphomas. An immunohistochemical antibody that specifically detects NUT protein overexpression can now facilitate rapid and cost-effective diagnosis of this rare tumor.<sup>12</sup> Experimental studies suggest that bromodomain inhibitors can drive terminal differentiation of NMC cells in culture and are thus a promising starting point for targeted inhibition of the BRD-NUT oncogenes.<sup>13</sup>

Although rare, NMC is likely seen at a higher frequency at referral cancer centers, due to potentially ambiguous diagnostic features and unusually aggressive clinical course. We retrospectively examined our consult files for cases diagnosed as primary pulmonary NMC and herein describe the clinical, radiographic, and pathologic features of eight cases identified between 2010 and 2014. In an effort to better understand the frequency of the NMC diagnosis in a more routine setting, we retrospectively screened in-house biopsies performed for lung cancer within our institution between 2002-2010, a period before screening of poorly differentiated carcinomas for NUT overexpression by IHC became commonplace in our practice. As a result of these efforts we demonstrate that primary pulmonary NMC, while rare, has highly characteristic symptomatic and radiographic features, pathology, and clinical course.

## Materials and Methods

### Case series

Following approval by the Brigham and Women's Hospital (BWH) Institutional Review Board (IRB), the pathology records of BWH were searched for the diagnosis "Nut midline carcinoma" associated with a biopsy or surgical resection obtained from the thoracic cavity. Tumors thought to arise at extrapulmonary sites (these included head and neck, kidney, and anterior mediastinum) were excluded from review. A total of eight cases were identified; all initially presented at an outside hospital and were reviewed in consultation at DFCI/BWH between 2010 and 2014. Pathology slides for all cases with material still available in the BWH archives were re-reviewed. Details of patient history and clinical course were derived from the electronic medical record.

### Radiology methods

The imaging studies at the time of diagnosis were reviewed by a board-certified radiologist with expertise in thoracic and oncologic imaging (M.N.). All but one patient had chest computed tomography (CT) scans available. Additional imaging studies, including <sup>18</sup>F fluorodeoxyglucose (FDG) positron emission tomography (PET)/CT, abdominal CT, head CT, bone scintigraphy, and brain magnetic resonance imaging (MRI), along with their radiology reports if available, were also reviewed if performed. Chest CT scans were evaluated focusing on the location and characteristics of the dominant lung lesion and associated lung parenchymal abnormalities, involvement of the contralateral lung, lymphadenopathy, pleural and osseous abnormalities. PET/CT and other imaging studies were reviewed to identify the involvement of extrathoracic sites.

### Screening cohort

The patient records at Dana Farber Cancer Institute (DFCI) were searched for all thoracic oncology patients with a biopsy performed for lung cancer at BWH between 2002-2010. The following diagnoses were included: poorly differentiated carcinoma, non-small cell lung carcinoma (NSCLC), squamous cell carcinoma, and high grade neuroendocrine carcinoma and/or small cell lung carcinoma. Study cases were further restricted to those with adequate formalin-fixed, paraffin-embedded tissue remaining in the archive. All specimens included in this study were obtained from patients who consented to correlative studies (DFCI IRB 02-180). Patient demographic and clinical features were derived from the medical record.

### Immunohistochemistry

IHC for NUT was performed on 4-micron-thick, formalin-fixed, paraffin-embedded (FFPE) sections. Slides underwent heat-induced epitope retrieval in citrate buffer and were incubated with primary rabbit monoclonal anti-NUT (clone C5261, 1:50) (Cell Signaling Technology, Danvers, MA) and visualized using Bond Polymer Refine Detection (Leica Microsystems, Buffalo Grove, IL). IHC staining for NUT was interpreted by 2 or more pathologists (S.P., L.M.S., and C.A.F.). Positivity was defined as strong, speckled nuclear staining in >50% of nuclei, as previously described.<sup>12</sup> Additional IHC staining for tumor markers was performed at the time of primary diagnosis according to standard clinical

operating procedures in the BWH immunohistochemistry laboratory. All tumors originally diagnosed as NSCLC were stained for this study with thyroid transcription factor-1 (TTF-1) (M3575, 1:300) (DAKO, Carpinteria, CA) and p40 (PC373; 1:800) (EMD Millipore, Billerica, MA). For both stains, antigen retrieval was carried out with citrate buffer in a pressure cooker.

### Fluorescence in situ Hybridization

Chromosomal translocation of the *NUT* gene locus was performed by FISH in NUT-IHC positive cases as previously described.<sup>14</sup> Dual-color split-apart FISH assays were carried out on 4-micron-thick FFPE tissue sections. *BRD4* on 19p13.1 was probed using telomeric tandem bacterial artificial chromosome (BAC) clones RP11-319o10 and RP11-681d10 (green) and centromeric BAC clones RP11-207i16 and CTD-3055m5 (red). *NUT* on 15q13 was probed using telomeric BAC clones 1H8 and 64o3B (green) and centromeric clones 1084a12 and 3d4 (red). Split apart of *NUT* and *BRD4* was deemed consistent with *BRD4-NUT* fusion. Dual-color bring-together FISH assays were carried out for detection of *BRD3-NUT* fusion on FFPE tissue sections. *BRD3* on 9q34.2 was probed using telomeric tandem bacterial artificial chromosome (BAC) clones RP11-145e17 and RP11-92b21 (red) and *NUT* was probed using telomeric BAC clones as above. Slides with >80% hybridization efficiency in 4 areas (200 cells/area) of the tissue section were considered interpretable.

## Results

### Case Series

The clinical, radiographic, and pathologic features of the eight patients identified with NMC in the institutional consultative practice are detailed in Tables 1 through 3. Selected radiographic, pathologic and/or molecular features of cases 3, 5, 6, 7 and 8 have been included in previous reports.<sup>1,13,15,16</sup> The mean age of the patients at the time of diagnosis was 41 years (median 30, range 21-68). Clinical history was available for 7 patients. Of these, six presented with a history of cough for one or months preceding their diagnosis and three complained of shoulder and/or flank pain. One patient had a long standing history of pipe smoking; all others were never or light smokers (Table 1). All were otherwise previously healthy.

Chest CT imaging was available for review in seven patients (Table 2). In all cases, the primary lung mass was centrally located, with a predilection for the lower lobes (5 of 7) and the right side (5 of 7). The primary tumor consistently presented as a large mass (range 5-11 cm in longest diameter) with irregular borders and low density components suggestive of necrosis and was confluent with ipsilateral hilar and mediastinal lymph nodes (Figure 1). Ipsilateral pleural disease was consistently present with pleural effusion in all cases, with accompanying pleural masses or thickening noted in 5 cases. The contralateral lung had no evidence of disease involvement on CT in all cases, other than trace or small pleural effusions in four cases. Regional adenopathy was similarly more pronounced on the side of the dominant mass and was noted in all cases; bilateral mediastinal lymphadenopathy was present in 4 cases, including 3 cases with bilateral supraclavicular nodal involvement. In 4 cases evaluated with PET/CT, all sites of tumor were intensely FDG-avid with SUVmax

measuring as high as 10 in some cases. In 2 of the cases with PET, central photopenia was noted in the lung mass suggesting necrosis. Definite bone involvement was seen in three patients, present as multiple lytic lesions on CT that were FDG-avid on PET/CT. In one case with multiple bone metastasis on PET and CT, bone scintigraphy was negative. Other distant sites of metastasis detected by CT and/or PET imaging included liver, subcutaneous soft tissue, and retroperitoneal lymph nodes. All cases were negative for brain metastases on imaging (5 cases with brain MRI and 2 cases with head CT).

Pathologic features are detailed in Table 3. Six of eight cases arrived in consultation with another suggested diagnosis, including NSCLC, not otherwise specified, adenosquamous carcinoma, thymic carcinoma, germ cell tumor, and lymphoma. Characteristic morphologic features included nested to sheetlike growth of a monomorphic proliferation of intermediate-sized round to epithelioid tumor cells with high nuclear:cytoplasmic ratio, open chromatin, variably prominent nucleoli, and small amounts of pale, amphophilic cytoplasm. Two cases showed multifocal crush artifact and nuclear molding, features most commonly associated with small cell carcinomas. One case, obtained from an extrapleural pneumonectomy specimen performed following chemotherapy, showed polygonal cells with prominent cherry-red nucleoli and more abundant pale, eosinophilic cytoplasm, raising a differential diagnosis of malignant melanoma (see Supplemental Figure 1).

One case originally classified as an adenosquamous carcinoma showed a population of primitive appearing cells with the cytomorphology described above admixed with a florid proliferation of columnar respiratory epithelial cells and a brisk polymorphonuclear infiltrate (see Supplemental Figure 2A). Immunohistochemistry showed that the primitive-appearing cells were diffusely p63 and NUT positive and the associated columnar cell proliferation (favored to represent a reactive population) was TTF-1 positive but p63 and NUT negative (see Supplemental Figure 2B, showing p63 staining in tumor cells; 2C, showing TTF-1 staining in reactive columnar cell proliferation and 2D, showing nuclear pattern of Nut protein expression in tumor cells; all panels at 400X). All cases in the series showed at least scattered p63 expression, and all cases showed at least focal cytokeratin expression. One tumor (case 8) showed discreet islands of keratinization by CK5/6 IHC. Interestingly, two cases, including one obtained from a supraclavicular lymph node biopsy (case 5; Figure 2A) showed focal (<10%), weak nuclear TTF-1 expression (Figure 2B). Neuroendocrine marker staining was performed in six cases and was focally positive in two (Table 3), including in one case with morphologic features of small cell carcinoma (Figure 2 panels C-D). MIB-1 proliferation index was 80-100% in two cases stained.

### Screening study

A total of 166 cases of in-house biopsies were successfully screened for NUT overexpression by immunohistochemistry. The original diagnoses are listed in Table 4. Based on recommendations that the diagnosis of NMC be considered only for non-gland forming epithelioid malignancies,<sup>8</sup> tumors diagnosed morphologically as adenocarcinoma were excluded from this study. Of this cohort, 54 were originally diagnosed as NSCLC. Additional immunohistochemistry using TTF-1 and p40 was performed to further subclassify these cases according to IASLC criteria,<sup>17</sup> with 31 reclassified as NSCLC, favor

adenocarcinoma, 8 reclassified as NSCLC, favor squamous cell carcinoma, and 15 remaining as NSCLC, not otherwise specified.

NUT overexpression was identified in one case (1 of 166 or 0.6%), in an endobronchial biopsy originally diagnosed as NSCLC, and reclassified as NSCLC, NOS based on scattered p63 positivity and focal (<10%) TTF-1 expression in the same cell population. Although this was a limited biopsy, it had features resembling those seen in the case illustrated in supplemental figure 2, with primitive-appearing round to epithelioid cells adjacent to a population of proliferative columnar epithelium and a brisk polymorphonuclear infiltrate (Figure 3A). NUT protein expression was confined to the primitive-appearing cells (Figure 3B). A BRD4-NUT translocation was confirmed by FISH (Figure 3C-D). This case was therefore reclassified as NMC. Notably, the patient from whom this biopsy was derived was a 29 year old woman with a 20-pack year history of smoking and a two month history of cough and fevers. CT and PET/CT imaging showed a large, FDG-avid mass (10 cm in diameter) located in the right middle lobe with post-obstructive atelectasis and small right pleural effusion, and bilateral hilar and mediastinal lymphadenopathy. No evidence of involvement was noted in the left lung, and no distant metastasis was noted on PET or on brain MRI. She was treated as stage IIIB squamous cell carcinoma (based on p63 positivity in a subsequent pleural biopsy) with carboplatin and taxol and radiation therapy, however she died of disease three months after her diagnosis.

## Discussion

Descriptions of primary pulmonary NMC have been limited to a few individual case reports or small case series,<sup>9-11,18</sup> as a result a clear clinicopathologic description of this entity is lacking. Our series is the largest reported to date and offers complete clinical, radiographic and pathologic detail for eight of the nine included patients.

The median age of diagnosis for lung cancers overall is 70 years, as compared to median of 30 (mean of 41) years in this cohort of NMC patients.<sup>19</sup> Overall, two patients had significant smoking history, but six had no or negligible tobacco exposure. At presentation, all patients complained of a month or more of cough and some had concurrent chest or shoulder pain. Despite the original descriptions of this entity in pediatric patients,<sup>20</sup> it is evident that older adults are not spared. Therefore, while NMC should always be included in the differential diagnosis of a malignant lung tumor presenting in a young person, it should also be considered in older adults, even those with a substantial smoking history, when the clinical course appears unusually aggressive.

Despite chemo- or chemoradiotherapy, all patients were dead of disease within 5 months. Interestingly, the survival time reported for NMC in the largest published series, including tumors arising at all sites, was 6.7 months,<sup>8</sup> whereas in our series of primary pulmonary NMC the median survival time was 2.2 months (66 days). While it is possible that primary pulmonary NMC are intrinsically more aggressive than NMC arising at other sites, the shorter survival time may simply reflect a relatively delayed onset of clinical symptoms for primary lung tumors as compared, for instance, to primary head and neck tumors, another common site of NMC presentation.

CT imaging of primary pulmonary NMC, while not necessarily specific, appears to have some characteristic features that are consistent across the cases in this study. All cases presented with a large primary lung mass (> 5cm in diameter) that was confluent with hilar and mediastinal adenopathy, often associated with post-obstructive atelectasis and ipsilateral pleural involvement. Notably, the contralateral lung was essentially spared in all cases. Bones were the most common site of extrathoracic involvement, with three of eight cases with available imaging showing definite bony metastases in the form of purely lytic lesions on CT scan, which were more easily detected on PET due to marked FDG avidity. In one case with multiple bone metastasis on PET and CT, bone scintigraphy was negative. This observation is consistent with other published reports and suggests that a negative bone scan may not reliably exclude metastases in this entity.<sup>15,21</sup> Eight patients had staging head imaging and all were negative for brain metastases. This is a notable observation, given that primary lung carcinomas have the highest incidence of brain metastases compared to other primary sites, with an incidence of nearly 30% in stage IV disease.<sup>22,23</sup> However, given that brain metastases have been observed in NMC,<sup>24</sup> the findings may be due to the fact that these patients did not live long enough to develop brain metastases.

The cytomorphology of NMC has been described extensively in the literature, and the appearance of the tumor cells in primary pulmonary NMC recapitulates that reported at other sites.<sup>6,7,25</sup> The histologic appearance may be readily confused with other high grade malignancies; in our series, other proposed diagnoses included lymphoma, germ cell tumor, and adenosquamous carcinoma, in addition to relatively nonspecific diagnoses such as poorly differentiated carcinoma or NSCLC. Additional considerations may be small cell carcinoma, in tumors with extensive crush artifact, or melanoma, in tumors with pronounced nucleoli, as we observed in a surgically resected NMC following neoadjuvant chemotherapy. Notably, two cases in this series showed focal CD56 and/or synaptophysin expression, findings that may further lead to a misdiagnosis of small cell carcinoma. In a recent series, two of eight patients diagnosed with small cell lung carcinoma under the age of 40 were retrospectively re-diagnosed with NMC based on positive NUT expression and rearrangement by FISH.<sup>26</sup> One tumor also showed subset positivity of CD56, highlighting the nonspecific character of neuroendocrine marker expression and the need to maintain a broad differential when diagnosing high grade carcinomas in young patients. In contrast to reports of NMC arising in the anterior mediastinum,<sup>7</sup> primary pulmonary NMC showed consistent keratin expression. Application of histone deacetylase inhibitors to NMC cells in vitro and in vivo drives them towards squamous differentiation.<sup>5</sup> In keeping with the hypothesis that NMC represents a subtype of squamous cell carcinoma all cases in our series showed at least scattered positivity for p63. From a diagnostic standpoint, it is important to note that three of the nine cases also had focal TTF-1 expression. TTF-1 with focal or multifocal p63 coexpression is not uncommon in lung tumors and favors the diagnosis of adenocarcinoma.<sup>27</sup> However, extensive p63/p40 expression with focal TTF-1 in the same tumor cell population is highly unusual among lung carcinomas and should bring NMC into consideration. The significance of TTF-1 expression in this tumor type is unclear; it may hint at the origin of primary pulmonary NMC from a pluripotent respiratory epithelial cell. Alternatively, it may simply represent aberrant TTF-1 expression similar to that reported in extrapulmonary small cell carcinomas.<sup>28</sup>

Given its rarity and likely underdiagnosis, the prevalence of NMC among patients with lung cancer is unknown. Based on the data from Haruki et al, one may conclude that this number is likely less than 1%.<sup>10</sup> Using a highly specific IHC-based screen of a cohort of consecutive diagnostic biopsies obtained at BWH, we retrospectively identified one primary pulmonary NMC among 166 tested cases of lung carcinoma lacking morphologic features of adenocarcinoma. This one case, from 2008, was diagnosed first as a NSCLC and on a subsequent biopsy as squamous cell carcinoma, based on p63 expression. Therefore, in this institutional series, primary pulmonary NMC similarly occurs in less than 1% of tumors that may be considered in the morphologic differential diagnosis.

In conclusion, we demonstrate that primary pulmonary NMC, while rare, has characteristic diagnostic features. In this case series, the stereotypical patient was otherwise healthy, typically with minimal smoking history, had a large burden of unilateral disease involving lung, pleura, and mediastinal lymph nodes, and a primitive tumor cell population showing keratin and p63 or p40 expression on biopsy. Tumors with these clinicopathologic and radiographic features should undergo screening with either NUT IHC and/or FISH. NMC of the lung is uniformly and rapidly lethal and thus prompt recognition is necessary to permit proper patient counseling and hopefully to eventually offer effective targeted therapy.

## Supplementary Material

Refer to Web version on PubMed Central for supplementary material.

## References

1. French CA, Rahman S, Walsh EM, et al. NSD3-NUT Fusion Oncoprotein in NUT Midline Carcinoma: Implications for a Novel Oncogenic Mechanism. *Cancer Discov.* 2014; 4:928–941. [PubMed: 24875858]
2. French CA. Pathogenesis of NUT midline carcinoma. *Annu Rev Pathol.* 2012; 7:247–265. [PubMed: 22017582]
3. French CA, Miyoshi I, Kubonishi I, et al. BRD4-NUT fusion oncogene: a novel mechanism in aggressive carcinoma. *Cancer Res.* 2003; 63:304–307. [PubMed: 12543779]
4. French CA, Ramirez CL, Kolmakova J, et al. BRD-NUT oncoproteins: a family of closely related nuclear proteins that block epithelial differentiation and maintain the growth of carcinoma cells. *Oncogene.* 2008; 27:2237–2242. [PubMed: 17934517]
5. Schwartz BE, Hofer MD, Lemieux ME, et al. Differentiation of NUT midline carcinoma by epigenomic reprogramming. *Cancer Res.* 2011; 71:2686–2696. [PubMed: 21447744]
6. Stelow EB, Bellizzi AM, Taneja K, et al. NUT rearrangement in undifferentiated carcinomas of the upper aerodigestive tract. *Am J Surg Pathol.* 2008; 32:828–834. [PubMed: 18391746]
7. Evans AG, French CA, Cameron MJ, et al. Pathologic characteristics of NUT midline carcinoma arising in the mediastinum. *Am J Surg Pathol.* 2012; 36:1222–1227. [PubMed: 22790861]
8. Bauer DE, Mitchell CM, Strait KM, et al. Clinicopathologic features and long-term outcomes of NUT midline carcinoma. *Clin Cancer Res.* 2012; 18:5773–5779. [PubMed: 22896655]
9. Tanaka M, Kato K, Gomi K, et al. NUT midline carcinoma: report of 2 cases suggestive of pulmonary origin. *Am J Surg Pathol.* 2012; 36:381–388. [PubMed: 22301500]
10. Haruki N, Kawaguchi KS, Eichenberger S, et al. Cloned fusion product from a rare t(15;19) (q13.2;p13.1) inhibit S phase in vitro. *J Med Genet.* 2005; 42:558–564. [PubMed: 15994877]
11. Parikh SA, French CA, Costello BA, et al. NUT midline carcinoma: an aggressive intrathoracic neoplasm. *J Thorac Oncol.* 2013; 8:1335–1338. [PubMed: 24457244]



12. Haack H, Johnson LA, Fry CJ, et al. Diagnosis of NUT midline carcinoma using a NUT-specific monoclonal antibody. *Am J Surg Pathol*. 2009; 33:984–991. [PubMed: 19363441]
13. Filippakopoulos P, Qi J, Picaud S, et al. Selective inhibition of BET bromodomains. *Nature*. 2010; 468:1067–1073. [PubMed: 20871596]
14. French CA, Kutok JL, Faquin WC, et al. Midline carcinoma of children and young adults with NUT rearrangement. *J Clin Oncol*. 2004; 22:4135–4139. [PubMed: 15483023]
15. Bair RJ, Chick JFB, Chauhan NR, et al. Demystifying NUT Midline Carcinoma: Radiologic and Pathologic Correlations of an Aggressive Malignancy. *Cardiopulmonary Imaging*. In Press.
16. Grayson AR, Walsh EM, Cameron MJ, et al. MYC, a downstream target of BRD-NUT, is necessary and sufficient for the blockade of differentiation in NUT midline carcinoma. *Oncogene*. 2014; 33:1736–1742. [PubMed: 23604113]
17. Travis WD, Brambilla E, Noguchi M, et al. Diagnosis of lung cancer in small biopsies and cytology: implications of the 2011 International Association for the Study of Lung Cancer/American Thoracic Society/European Respiratory Society classification. *Arch Pathol Lab Med*. 2013; 137:668–684. [PubMed: 22970842]
18. Dang TP, Gazdar AF, Virmani AK, et al. Chromosome 19 translocation, overexpression of Notch3, and human lung cancer. *J Natl Cancer Inst*. 2000; 92:1355–1357. [PubMed: 10944559]
19. Howlander, N.; Noone, AM.; Krapcho, M., et al. SEER Cancer Statistics Review, 1975-2011, National Cancer Institute. Bethesda, MD: 2014. Available at: [http://seer.cancer.gov/csr/1975\\_2011/](http://seer.cancer.gov/csr/1975_2011/). Accessed August 22, 2014
20. Kubonishi I, Takehara N, Iwata J, et al. Novel t(15;19)(q15;p13) chromosome abnormality in a thymic carcinoma. *Cancer Res*. 1991; 51:3327–3328. [PubMed: 2040007]
21. Rosenbaum DG, Teruya-Feldstein J, Price AP, et al. Radiologic features of NUT midline carcinoma in an adolescent. *Pediatr Radiol*. 2012; 42:249–252. [PubMed: 22057302]
22. Barnholtz-Sloan JS, Sloan AE, Davis FG, et al. Incidence proportions of brain metastases in patients diagnosed (1973 to 2001) in the Metropolitan Detroit Cancer Surveillance System. *J Clin Oncol*. 2004; 22:2865–2872. [PubMed: 15254054]
23. Schouten LJ, Rutten J, Huvneers HA, et al. Incidence of brain metastases in a cohort of patients with carcinoma of the breast, colon, kidney, and lung and melanoma. *Cancer*. 2002; 94:2698–2705. [PubMed: 12173339]
24. Polsani A, Braithwaite KA, Alazraki AL, et al. NUT midline carcinoma: an imaging case series and review of literature. *Pediatr Radiol*. 2012; 42:205–210. [PubMed: 22033856]
25. Bellizzi AM, Bruzzi C, French CA, et al. The cytologic features of NUT midline carcinoma. *Cancer*. 2009; 117:508–515. [PubMed: 19795508]
26. Taniyama TK, Nokihara H, Tsuta K, et al. Clinicopathological features in young patients treated for small-cell lung cancer: significance of immunohistological and molecular analyses. *Clin Lung Cancer*. 2014; 15:244–247. [PubMed: 24456892]
27. Rekhman N, Ang DC, Sima CS, et al. Immunohistochemical algorithm for differentiation of lung adenocarcinoma and squamous cell carcinoma based on large series of whole-tissue sections with validation in small specimens. *Mod Pathol*. 2011; 24:1348–1359. [PubMed: 21623384]
28. Agoff SN, Lamps LW, Philip AT, et al. Thyroid transcription factor-1 is expressed in extrapulmonary small cell carcinomas but not in other extrapulmonary neuroendocrine tumors. *Mod Pathol*. 2000; 13:238–242. [PubMed: 10757334]

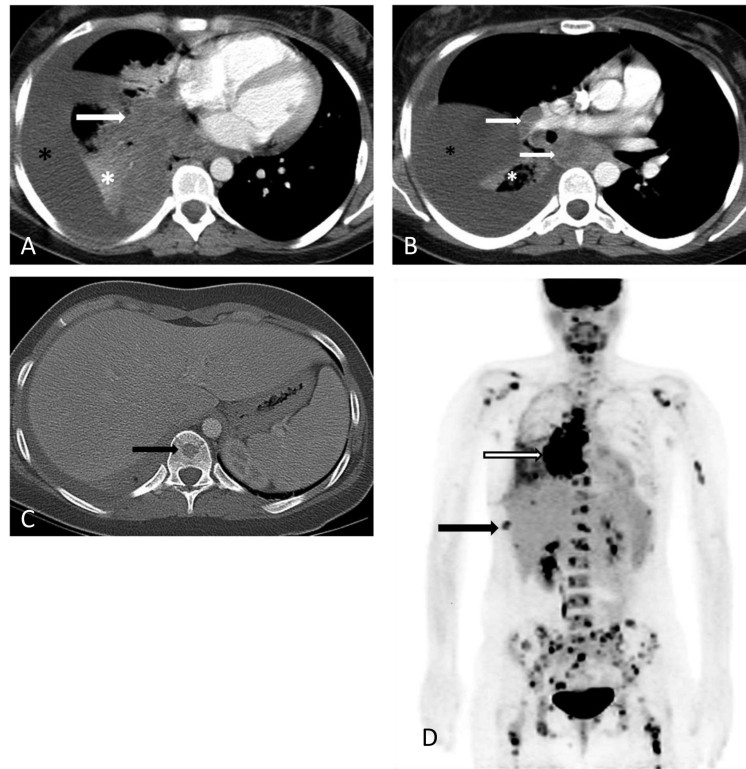


**Figure 1.**

Contrast enhanced CT scan of the chest demonstrated a large, poorly-defined mass in the right lower lobe (arrow, panel A), located centrally and confluent with right hilar and mediastinal adenopathy (arrows, panel B). Note right pleural effusion (black asterisk, panel A) and obstructive atelectasis on the right (white asterisk, panel A). There was no evidence of involvement of the left lung. Bone metastasis was present, demonstrating lytic lesions (black arrow, panel C). Whole body image of the FDG-PET scan demonstrated marked FDG avidity of the dominant lung lesion (white arrow, panel D), as well as metastatic sites including innumerable osseous lesions and a subcutaneous lesion in the right flank (black arrow, panel D). Most of the osseous lesions were more noticeable on PET than CT, and Tc-99m MDP bone scintigraphy was negative for osseous metastasis.

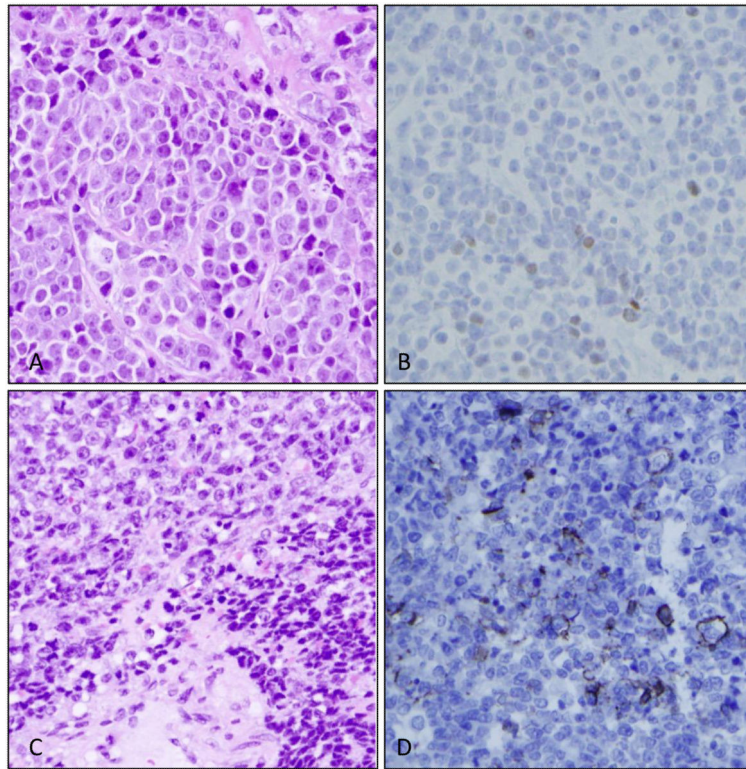


**Figure 2.**

A) Hematoxylin and eosin stain (400X) of a Nut midline carcinoma showing B) weak, scattered nuclear positivity for thyroid transcription factor-1 (TTF-1). C) Hematoxylin and eosin stain (200X) of a Nut midline carcinoma with crush artifact and nuclear molding (lower right) and B) scattered tumor cells with membranous CD56 expression.

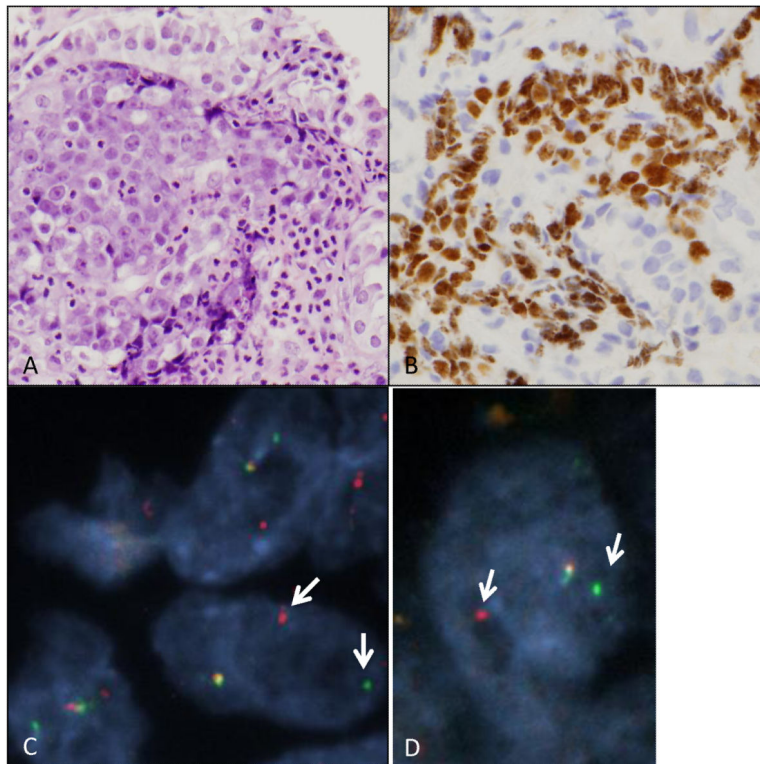


**Figure 3.** Retrospectively identified primary pulmonary Nut midline carcinoma. A) Hematoxylin and eosin-stained slide at 400X showing a primitive cell population surrounded by a proliferation of reactive respiratory epithelial cells and marked neutrophilic infiltrate. B) NUT immunohistochemistry is positive in the primitive-appearing cells. C) Dual color FISH using probes flanking the *NUT* locus shows split-apart of red and green signals (white arrows) consistent with *NUT* rearrangement. D) Dual color FISH using probes flanking the *BRD4* locus shows split-apart of red and green signals (white arrows) consistent with *BRD4* rearrangement. Together with Fig. 3C, the findings are consistent with a *BRD4-NUT* fusion.

**Table 1**

Clinical features of patients diagnosed with primary pulmonary NUT Midline Carcinoma

Case #	Age	Sex	Tobacco history	Presenting sx	Treatment	Outcome	Survival time (months)	References
1	68	F	unknown	unknown	unknown	Death	1	none
2	21	F	Never	Right flank and shoulder pain, cough × 1 month	Chemotherapy	Death	4	none
3	23	M	2 pack years	Cough × 2 mos	Chemotherapy Extrapleural pneumonectomy	Death	2	Bair et al., AJR 2014
4	63	F	Never	Cough × 6mos, right chest/back/shoulder pain	Chemotherapy	Death	2	none
5	37	M	Never	Cough × 3mos	Chemotherapy	Death	1	French et al.. Cancer Discovery 2014
6	63	M	Pipe smoker, 40 years	Dyspnea, cough, hemoptysis × 2 mos	--	Death	1	Bair et al., AJR 2014
7	26	M	Never	Fever, URI × 2 mos	Chemotherapy	Death	2	Bair et al., AJR 2014
8	30	M	3 pack years	Shoulder pain, cough with hemoptysis × 1 month	Chemotherapy	Death	5	Bair et al., AJR 2014 Filippakopoulos et al. Nature. 2010 Grayson et al.. Oncogene 2014
9	29	F	20 pack years	Cough, fever × 2 mos	Chemotherapy, radiation	Death	3	none

Radiographic features of primary pulmonary Nut midline carcinoma

Table 2

Case#	Site	Size (cm)	Lung	Pleura	Contralateral lung involvement	Lymphadenopathy	Extrathoracic sites	PET
1								
No images								
2	RLL, central	5×5	Post-obstructive atelectasis	Large effusion Pleural nodule	None	Mediastinal Subcarinal Hilar(R) +necrosis	Subcutis, bone	Intensely FDG avid, including bone and soft tissue metastases
3	RLL, central	11×6	Post-obstructive atelectasis	Large effusion, Pleural nodules with central necrosis	Small left- sided effusion	Mediastinal Subcarinal Hilar(R) +necrosis	None detected	Intensely FDG avid with central photopenia
4	RUL, central	8×5	Post-obstructive atelectasis, Lymphangitic spread	Small effusion	None	Supraclavicular Hilar Mediastinal Axillary (B)	(R) retrocrural & aorto-caval nodes, Bone	Intensely FDG avid
5	RLL, central	7×4	Post-obstructive atelectasis	Large effusion Pleural thickening	Trace left effusion	Supraclavicular Hilar Mediastinal(B) Paraesophageal(L)	Liver, bone	N/A
6	LUL, central	11×10	Post-obstructive atelectasis, Lymphangitic spread	Large effusion Pleural nodules	Small right effusion	Supraclavicular Mediastinal(B) Hilar(L)	None detected	N/A
7	RLL, central	9×8	Post-obstructive atelectasis	Small right effusion	Trace left effusion	Mediastinal Subcarinal Hilar(R)	None detected	Intensely FDG avid with central photopenia
8	LLL, central	8×6	Post-obstructive atelectasis	Moderate effusion Pleural nodules	none	Mediastinal(B) Subcarinal Hilar(L) + necrosis	Liver, bone	N/A
9	RML	10×10	Post-obstructive atelectasis	Small right effusion	None	Hilar (B) Mediastinal (B)	None	Intensely FDG avid

RLL = right lower lobe, RUL = right upper lobe, LUL = left upper lobe, LLL = left lower lobe, N/A = not available , B = bilateral

Table 3

## Pathologic features of primary pulmonary NUT midline carcinoma

Case #	Suggested diagnosis	P63 expression	TTF-1 expression	Keratin expression	Neuroendocrine marker expression	NUT IHC result	FISH result
1	Lymphoma	Diffuse	Negative	MNF-116 (focal)	Negative for synaptophysin, chromogranin, and CD56	Positive	<i>BRD4-NUT</i> fusion
2	Nut midline carcinoma	Scattered cells	ND	Pan-K, Cam5.2	ND	Positive	<i>BRD4-NUT</i> fusion
3	Thymic carcinoma	Multifocal	Negative	AE1/AE3(focal)	ND	Positive	<i>BRD4-NUT</i> fusion
4	Poorly differentiated NSCLC	Focal*	Focal	AE1/AE3, CK5/6, CK7 (focal), CK20 (focal)	Negative for synaptophysin, chromogranin	Positive	Variant NUT rearrangement
5	Germ cell tumor	Multifocal to Diffuse	Focal	Cam5.2, AE1/AE3(focal)	Positive for CD56 (focal) Negative for synaptophysin, chromogranin	Positive	<i>BRD4-NUT</i> fusion
6	Nut midline carcinoma	Diffuse	Negative	CK7 (focal), CK20 (focal), CK5/6(focal)	Negative for synaptophysin, chromogranin, and CD56	Positive	<i>BRD3-NUT</i> fusion
7	Adenosquamous carcinoma	Diffuse	Negative	Cam 5.2, AE1/AE3(focal), CK5/6 (focal)	Negative for synaptophysin	Positive	<i>BRD4-NUT</i> fusion
8	Poorly differentiated carcinoma	Diffuse	Negative	Cam5.2, AE1/AE3	Positive for synaptophysin (focal) Negative for chromogranin	Positive	<i>BRD4-NUT</i> fusion
9	NSCLC	Scattered	Focal	ND	ND	Positive	<i>BRD4-NUT</i> fusion

ND = not done; NSCLC = non small cell lung carcinoma; Pan-K = Pan-cytokeratin, CK7 = cytokeratin 7, CK20 = cytokeratin 20; CK5/6 = cytokeratin 5/6; TTF-1 = thyroid transcription factor-1

\* p40 was also examined in this case and was positive.

**Table 4**

Diagnoses of lung cancer cases screened by Nut immunohistochemistry.

Diagnosis	Number
Squamous cell carcinoma (SQC)	
Morphologic SQC	66
NSCLC, favor SQC	8
Adenocarcinoma (ADC)	
ADC, poorly differentiated	3
NSCLC, favor ADC	31
Adenosquamous carcinoma	4
Undifferentiated carcinoma	
NSCLC, not otherwise specified	15
Poorly differentiated carcinoma	4
Large cell carcinoma	2
Neuroendocrine carcinoma	
Small cell lung carcinoma (SCLC)	25
Large cell neuroendocrine carcinoma (LCNEC)	4
combined SCLC/LCNEC	2
combined SCLC/NSCLC	2
Total	166

Author Manuscript

Author Manuscript

Author Manuscript

Author Manuscript